Synthesis and properties of ferroelectric Si-doped (Bi, Nd)$_4$Ti$_3$O$_{12}$ thin films by chemical solution deposition

**Wataru Sakamoto · Yu-ki Mizutani · Naoya Iizawa ·
Toshinobu Yogo · Takashi Hayashi · Shin-ichi Hirano**

Abstract Ferroelectric Si-doped (Bi,Nd)$_4$Ti$_3$O$_{12}$ thin films have been prepared on Pt/TiO$_x$/SiO$_2$/Si substrates through metal-organic compounds by the chemical solution deposition. The Bi$_{3.25}$Nd$_{0.75}$Ti$_{2.9}$Si$_{0.1}$O$_{12}$ (BNTS) precursor films were found to crystallize into the Bi-layered perovskite Bi$_4$Ti$_3$O$_{12}$ single-phase above 600°C. The synthesized BNTS films revealed a random orientation having a strong 117 reflection. The BNTS thin films prepared between 600°C and 700°C showed well-saturated *P-E* hysteresis loops with P_r of 13–14 μC/cm^2 and E_c of 100–110 kV/cm at an applied voltage of 5 V. The surface roughness of the BNTS thin films was improved by Si doping compared with that of undoped Bi$_{3.35}$Nd$_{0.75}$Ti$_3$O$_{12}$ films.

Keywords (Bi,Nd)$_4$Ti$_3$O$_{12}$ · Si doping · Chemical solution deposition · Thin film · Ferroelectric properties

1 Introduction

Bismuth-layered structure ferrelectrics, such as Bi$_4$Ti$_3$O$_{12}$ (BiT), are promising candidates of lead-free ferroelectric materials and their thin films have been receiving great attention for their potential applications in nonvolatile ferroelectric random access memories (FeRAMs). Among several Bi-layered perovskite compounds, BiT thin films are known to have a large remanent polarization (P_r), a high Curie temperature and lower crystallization temperatures. However, BiT contains volatile Bi ions which are easily evaporated during heating. The volatility of Bi ions affects the formation of oxygen vacancies which leads to degrade the ferroelectric properties of resultant thin films. Bi^{3+} ions in the BiT structure can be substituted by nonvolatile rare earth ions for the improvement of its properties. Rare-earth-modified BiT thin films has been intensively studied as a ferroelectric layer for memory devices because of its excellent properties [1–6]. However, the fabrication of high-density FeRAMs is still difficult, because of problems such as insufficient microstructure and ferroelectric properties. Recently, silicon (Si)-substituted BiT thin films with good surface morphologies were reported by Kijima et al. [7]. Also, the authors demonstrated that chemically derived Nd-substituted BiT (BNT) thin films showed larger ferroelectricity than the other rare-earth-ion-substituted BiT thin films [5]. Therefore, Si-doped BNT thin films are expected to exhibit excellent ferroelectric properties with a good surface morphology.

As a fabrication method of thin film, the chemical solution deposition (CSD) process using metal-organic compounds is useful for the precise control of the chemical composition of desired thin films with reducing the processing temperature and equipment costs. This paper describes the synthesis of Bi-layered perovskite (Bi$_{3.25}$Nd$_{0.75}$)(Ti$_{2.9}$Si$_{0.1}$)O$_{12}$ (BNTS) thin films through the CSD method using metal-organic precursor solutions. The effects of Si doping to (Bi,Nd)$_4$Ti$_3$O$_{12}$ on the crystallization of precursor films and the surface morphology of crystallized films were examined. The ferroelectric properties of the BNTS films were also discussed.

W. Sakamoto (✉) · Y.-k. Mizutani · T. Yogo
Division of Nanomaterials Science, EcoTopia Science Institute,
Nagoya University, Furo-cho, Chikusa-ku, Nagoya 464-8603,
Japan
e-mail: sakamoto@esi.nagoya-u.ac.jp

N. Iizawa · T. Hayashi
Department of Materials Science and Engineering,
Shonan Institute of Technology, 1-1-25 Tsujido-Nishikaigan,
Fujisawa, Kanagawa 251-8511, Japan

S.-i. Hirano
Department of Applied Chemistry, Graduate School of
Engineering, Nagoya University, Furo-cho, Chikusa-ku, Nagoya
464-8603, Japan

2 Experimental procedures

$Bi(O^tC_5O_{11})_3$, $Ti(O^iC_3H_7)_4$ [Kojundo Chemical, Japan], $Si(OC_2H_5)_4$ [Kishida Chemical, Japan] and $Nd(CH_3COO)_3 \cdot H_2O$ [Mitsuwa Chemical, Japan] were used as starting materials for the preparation of $(Bi,Nd)_4(Ti,Si)_3O_{12}$ precursor solutions. $Nd(CH_3COO)_3 \cdot H_2O$ was heated at 110°C under vacuum for 4 h, yielding anhydrous $Nd(CH_3COO)_3$. 2-Methoxyethanol as a solvent was dried over a molecular sieve and distilled prior to use. The required amounts of $Bi(O^tC_5O_{11})_3$, $Ti(O^iC_3H_7)_4$, dehydrated $Nd(CH_3COO)_3$ and $Si(OC_2H_5)_4$ corresponding to a $Bi_{3.35}Nd_{0.75}Ti_{2.9}Si_{0.1}O_{12}$ (BNTS) composition (with 3% of excess Bi) were dissolved in absolute 2-methoxyethanol, and acetylacetone was then added to the solution as a stabilizing agent. The molar ratio of acetylacetone to BNTS precursor was 6. Since the starting materials are extremely sensitive to moisture, the entire procedure was carried out in a dry N_2 atmosphere. The solution was refluxed for 18 h, yielding a homogeneous solution. The precursor solutions were concentrated to approximately 0.1 mol/l by the removal of the solvent by vacuum evaporation.

Precursor films were prepared using the BNTS precursor solutions by spin-coating on Pt(200 nm)/TiO$_x$ (50 nm)/SiO$_2$/Si substrates. As-deposited precursor films were dried on a hot plate at 150°C for 5 min, and then calcined at 500°C for 10 min in an O_2 flow followed by crystallization between 600°C and 700°C for 30 min at a rate of 150°C/min using rapid thermal annealing (RTA) in an O_2 flow. The thickness of BNTS films was adjusted to be approximately 100 nm by repeating the coating/calcining cycle.

Powder sample was also prepared from the precursor solution by the removal of the solvent to study the crystallization of the BNTS precursor. The precursor powder was heat-treated at 800°C in an O_2 flow for 1 h.

The crystallographic phases of the powders and the thin films on substrates were characterized by X-ray diffraction (XRD) analysis using CuKα radiation with a monochromator and by Raman microprobe spectroscopy. The surface morphology of the synthesized films was observed using an atomic force microscope (AFM). After film fabrication, platinum top electrodes were deposited onto the surface of the films by RF sputtering for electrical measurement, followed by annealing at the crystallization temperature for 30 min. The ferroelectric properties of the films were evaluated using a ferroelectric test system at 100 Hz and room temperature.

3 Results and discussion

3.1 Crystallization of BNTS precursor powders and thin films

In this study, the amounts of Nd for the Bi site of $(Bi,Nd)_4(Ti,Si)_3O_{12}$ and excess Bi were set at the same
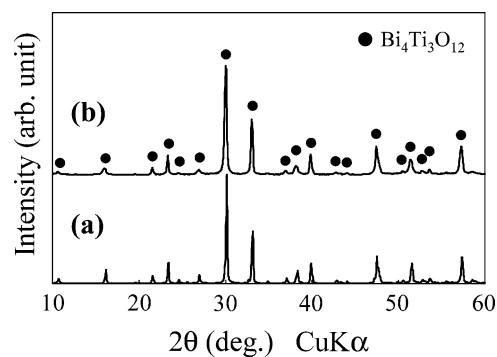
Fig. 1 XRD patterns of (a) $Bi_{3.35}Nd_{0.75}Ti_3O_{12}$ (BNT) and (b) $Bi_{3.35}Nd_{0.75}Ti_{2.9}Si_{0.1}O_{12}$ (BNTS) powders crystallized at 800°C

values as those in the previous works [3, 5, 6]. The Si amount of $(Bi,Nd)_4(Ti,Si)_3O_{12}$ was determined based upon the most effective amount of Ge for $(Bi,Nd)_4(Ti,Ge)_3O_{12}$ thin films reported by the authors [8, 9]. The crystallization of $Bi_{3.35}Nd_{0.75}Ti_{2.9}Si_{0.1}O_{12}$ (BNTS) precursor powder was investigated prior to the synthesis of ferroelectric Bi-layered perovskite BNTS films. Figure 1 illustrates XRD profiles of $Bi_{3.35}Nd_{0.75}Ti_3O_{12}$ (BNT) and BNTS precursor powders after heat treatment at 800°C. In order to clarify the effect of Si doping in the $Bi_4Ti_3O_{12}$ (BiT) structure on the crystallographic phase of resultant powders, the crystallization temperature was selected to be 800°C. The BNT and BNTS precursor powders were found to crystallize in the single-phase BiT, because no diffraction corresponding to the second phase was observed. Further characterization for the crystallographic phase of BNTS powders was carried out by Raman spectroscopy. Figure 2 shows Raman spectra of BNT and BNTS powders heat-treated at 800°C. The Raman spectrum of BNTS was in good agreement with that of BNT. The characteristic Raman scatterings of BNT were assigned
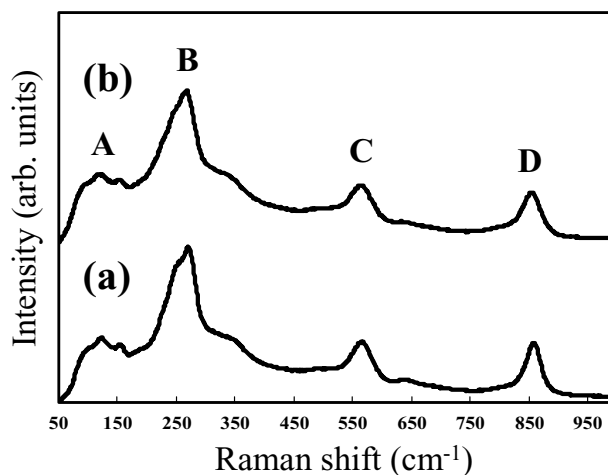
Fig. 2 Raman spectra of crystalline (a) BNT and (b) BNTS powders prepared at 800°C. [A: Vibration of Bi (A site)-O bonds, B: TiO$_6$ stretching and vibration modes, C: Vibration in a pseudo-perovskite layer, D: Vibration of Bi (A site)-O bonds]
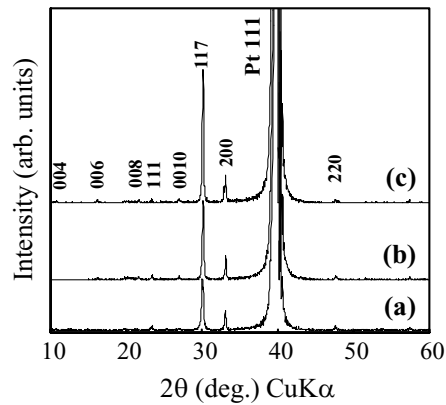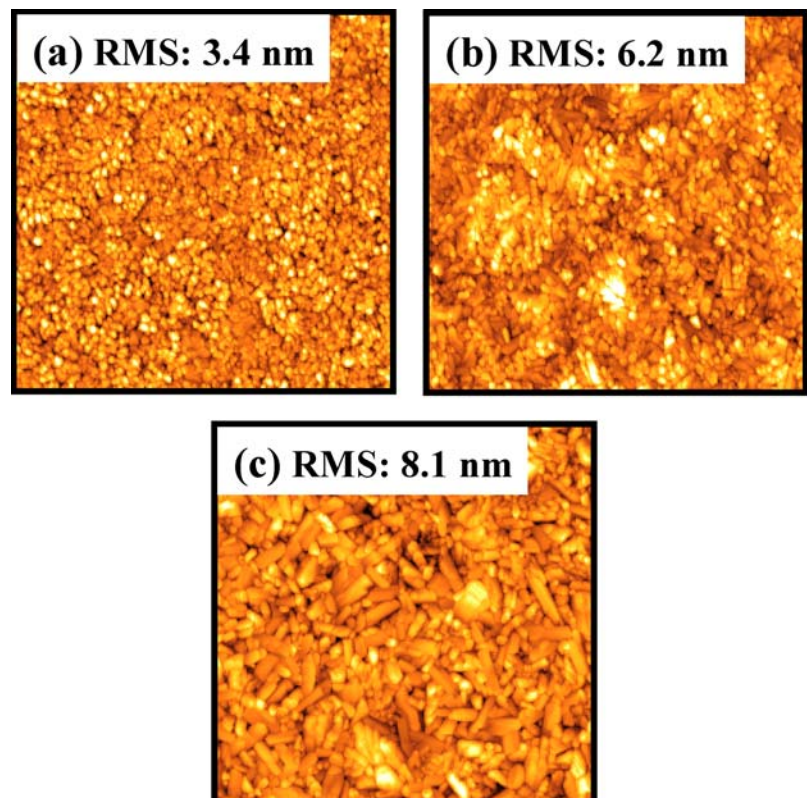
Fig. 3 XRD profiles of $Bi_{3.35}Nd_{0.75}Ti_{2.9}Si_{0.1}O_{12}$ (BNTS) thin films on Pt/TiO$_x$/SiO$_2$/Si substrates crystallized at (a) 600°C, (b) 650°C and (c) 700°C

to the same modes reported for $(Bi,La)_4Ti_3O_{12}$ [10] from A to D as shown in Fig. 2. No scattering of Bi-Si-O compound, such as $Bi_4Si_3O_{12}$ [11] was observed for the BNTS powder shown in Fig. 2(b). It turned out from Figs. 1 and 2 that BNTS precursor powder was confirmed to crystallize in the BiT structure of single-phase BNT.

Figure 3 illustrates the XRD profiles of BNTS thin films prepared between 600°C and 700°C on Pt/TiO$_x$/SiO$_2$/Si substrates. These films crystallized into the BiT single phase and exhibited a random orientation with a strong 117 reflection, because no change in diffractions with Si doping was
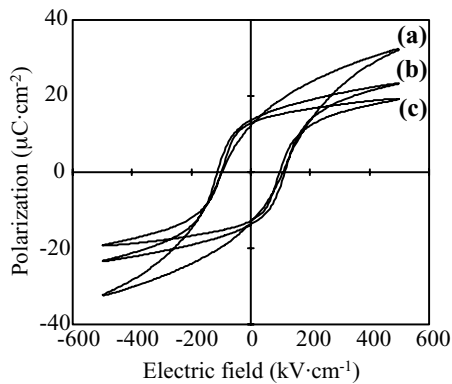
observed, as shown in Figs. 3(a)–(c). These films were also found to exhibit the same Raman spectra as powders shown in Fig. 2.

3.2 Surface morphology of BNTS thin films

Figure 4 shows AFM surface images of BNTS thin films prepared between 600°C and 700°C on Pt/TiO$_x$/SiO$_2$/Si substrates. The root mean square (RMS) roughness of the BNTS thin films prepared at 700°C was about 8.1 nm. In addition, BNTS thin films prepared below 700°C showed lower RMS values. The RMS values of the BNTS thin films prepared at 650 and 600°C were measured to be 6.2 and 3.4 nm, respectively. These RMS roughness values were smaller than those of undoped BNT thin films [9]. Also, the grain size of the BNTS thin films were found to be relatively small compared with those of reported undoped BNT thin films prepared by the CSD [12]. As can be seen from Fig. 4, the nucleation and growth process in the BNTS thin film during heating could be changed by doping of Si for the BNT. This result is important in fabricating thinner ferroelectric layers for electronic devices with low working voltages.
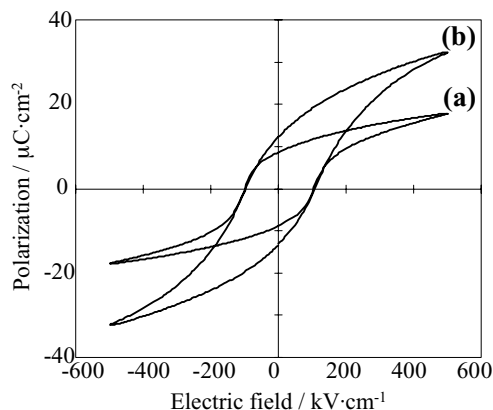
3.3 Ferroelectric properties of BNTS thin films

Figure 5 shows *P-E* hysteresis loops of the BNTS thin films crystallized at between 600°C and 700°C. These films are
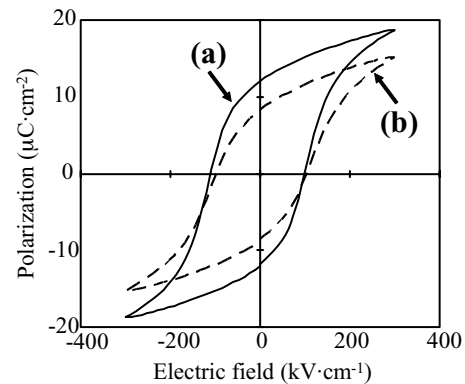
Fig. 4 AFM images of the surfaces of BNTS thin films on Pt/TiO$_x$/SiO$_2$/Si substrates prepared at (a) 600°C, (b) 650°C and (c) 700°C

Fig. 5 P-E hysteresis loops of the BNTS thin films on Pt/TiO$_x$/SiO$_2$/Si substrates prepared at (a) 600°C, (b) 650°C and (c) 700°C

Fig. 7 P-E hysteresis loops of BNTS thin film on Pt/TiO$_x$/SiO$_2$/Si substrate prepared at 650°C (a) before and (b) after fatigue measurement of 10^{10} switching cycles at a frequency of 1 MHz

approximately 100 nm in thickness. *P-E* hysteresis measurements were performed at an applied voltage of 5 V and a frequency of 100 Hz. The remanent polarization (P_r) and coercive field (E_c) of BNTS thin films prepared at 700°C were 13 μC/cm^2 and 99 kV/cm, respectively. On the other hand, BNTS thin films prepared at 650°C exhibited a little higher P_r value of 14 μC/cm^2 with a E_c of 110 kV/cm. At lower crystallization temperature of 600°C, the P_r of BNTS thin films was 13 μC/cm^2, which value was higher than that of BNT thin films (9.0 μC/cm^2) fabricated by the same process as shown in Fig. 6. The reported P_r value of BNT at 700°C (about 20 μC/cm^2) was larger than that of BNTS at 700°C [6, 12]. However, the P_r does not decrease in Si-doped BNT films, even when the crystallization temperature is lowered by 50–100°C. This tendency is consistent with Ge-doped (Bi,Nd)$_4$Ti$_3$O$_{12}$ thin films [8, 9]. The lower P_r value of BNT thin films at lower temperatures might be due to the inhomogeneous bimodal grain microstructure as reported by the authors [9]. On the other hand, BNTS thin films at 600–700°C had dense and improved surface roughness (Fig. 4). Applied voltages onto the BNTS films may be adequately worked in case of *P-E* hysteresis measurements. The surface

morphology and ferroelectric properties will be improved by the further control of synthesis conditions such as optimization of the Si content in BNTS, particularly for the case of thinner films prepared at lower temperatures.

3.4 Fatigue properties of BNTS thin films

Figure 7 shows *P-E* hysteresis loops of BNTS thin film prepared at 650°C before and after 10^{10} switching cycles at a frequency of 1 MHz under an applied voltage of 3 V. In the case of BNTS thin film prepared at 650°C, well-saturated *P-E* hysteresis loops were observed even at 3 V. The P_r values of the BNTS thin film decreased by about 30% after the fatigue measurement of 10^{10} cycles (Fig. 7(b)). The fatigue of the BNTS thin film was found to begin at around 10^8 cycles. BNT thin films prepared at 700°C also exhibited similar fatigue endurance to the BNTS film shown in Fig. 7. The fatigue phenomena of the current films may be improved by further V doping with higher valence to eliminate the defects in the thin films such as oxygen vacancy as in the case for the (Bi,Nd)$_4$Ti$_3$O$_{12}$ thin films [13].

4 Conclusions

Ferroelectric Si-doped (Bi,Nd)$_4$Ti$_3$O$_{12}$ thin films were successfully synthesized from metal-organic precursor solutions, and their crystallographic phase, crystal orientation, microstructure and ferroelectric properties were examined. Bi$_{3.35}$Nd$_{0.75}$Ti$_{2.9}$Si$_{0.1}$O$_{12}$ precursor films on Pt/TiO$_x$/SiO$_2$/Si substrates crystallized into the layered perovskite Bi$_4$Ti$_3$O$_{12}$ single-phase above 600°C with 117 preferred orientation. The Si doping to Bi$_{3.35}$Nd$_{0.75}$Ti$_3$O$_{12}$ was found to improve the surface roughness of resultant films. Si-doped Bi$_{3.25}$Nd$_{0.75}$Ti$_3$O$_{12}$ thin films exhibited well-saturated *P-E* hysteresis loops with P_r values larger than 10 μC/cm^2 even at an applied voltage of 3 V. Si-doped (Bi,Nd)$_4$Ti$_3$O$_{12}$ thin

Fig. 6 P-E hysteresis loops of (a) BNT and (b) BNTS thin films on Pt/TiO$_x$/SiO$_2$/Si substrates prepared at 600°C

films developed in this study have a potential for application in the ferroelectric layer of thin film electronic devices, such as FeRAM, with low working voltages.

References

1. B.H. Park, B.S. Kang, S.D. Bu, T.W. Noh, J. Lee, and W. Joe, *Nature*, **401**, 682 (1999).
2. D. Wu, A. Li, T. Zhu, Z. Li, Z. Liu, and N. Ming, *J. Mater. Res.*, **16**, 1325 (2001).
3. T. Hayashi, D. Togawa, M. Yamada, W. Sakamoto, and S. Hirano, *Jpn. J. Appl. Phys.*, **41**, 6814 (2002).
4. T. Kojima, T. Watanabe, H. Funakubo, K. Saito, M. Osada, and M. Kakihana, *J. Appl. Phys.*, **93**, 1707 (2003).
5. M. Yamada, N. Iizawa, T. Yamaguchi, W. Sakamoto, K. Kikuta, T. Yogo, T. Hayashi, and S. Hirano, *Jpn. J. Appl. Phys.*, **42**, 5222 (2003).
6. W. Sakamoto, M. Yamada, N. Iizawa, Y. Mizutani, D. Togawa, K. Kikuta, T. Yogo, T. Hayashi, and S. Hirano, *J. Electroceram.*, **13**, 339 (2004).
7. T. Kijima and H. Ishiwara, *Jpn. J. Appl. Phys.*, **41**, L716 (2002).
8. W. Sakamoto, Y. Mizutani, N. Iizawa, T. Yogo, T. Hayashi, and S. Hirano, *Jpn. J. Appl. Phys.*, **42**, L1384 (2003).
9. W. Sakamoto, Y. Mizutani, N. Iizawa, T. Yogo, T. Hayashi, and S. Hirano, *Jpn. J. Appl. Phys.*, **43**, 6599 (2004).
10. M. Osada, M. Tada, M. Kakihana, T. Watanabe, and H. Funakubo, *Jpn. J. Appl. Phys.*, **40**, 5572 (2001).
11. P. Beneventi, D. Bersani, P.P. Lottici, and L. Kovacs, *Solid State Comm.*, **93**, 143 (1995).
12. T. Hayashi, N. Iizawa, D. Togawa, M. Yamada, W. Sakamoto, and S. Hirano, *Jpn. J. Appl. Phys.*, **42**, 1660 (2003).
13. T. Hayashi, N. Iizawa, D. Togawa, M. Yamada, W. Sakamoto, K. Kikuta, T. Yogo, and S. Hirano, *Integrated Ferroelectr.*, **62**, 233 (2004).